Figure S1

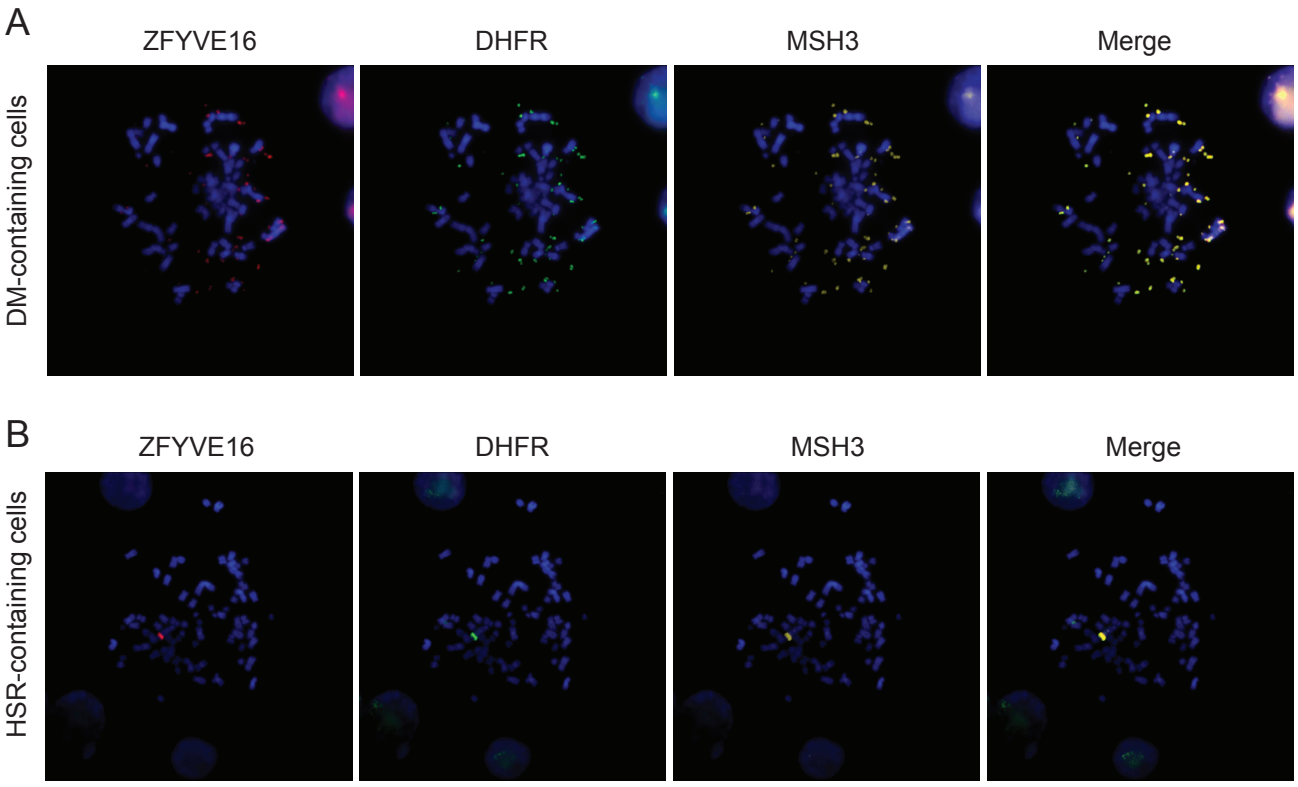
A
ZFYVE16
DHFR
MSH3
Merge
DM-containing cells
B
ZFYVE16
DHFR
MSH3
Merge
HSR-containing cells

Figure S2

A

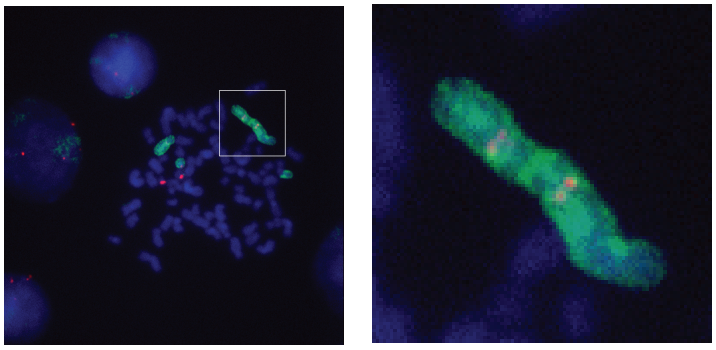

B

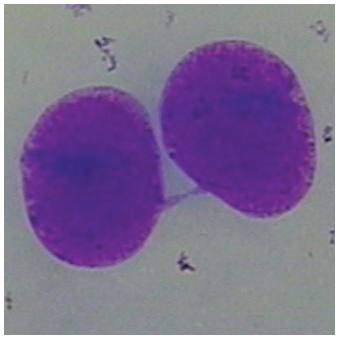

Figure S3

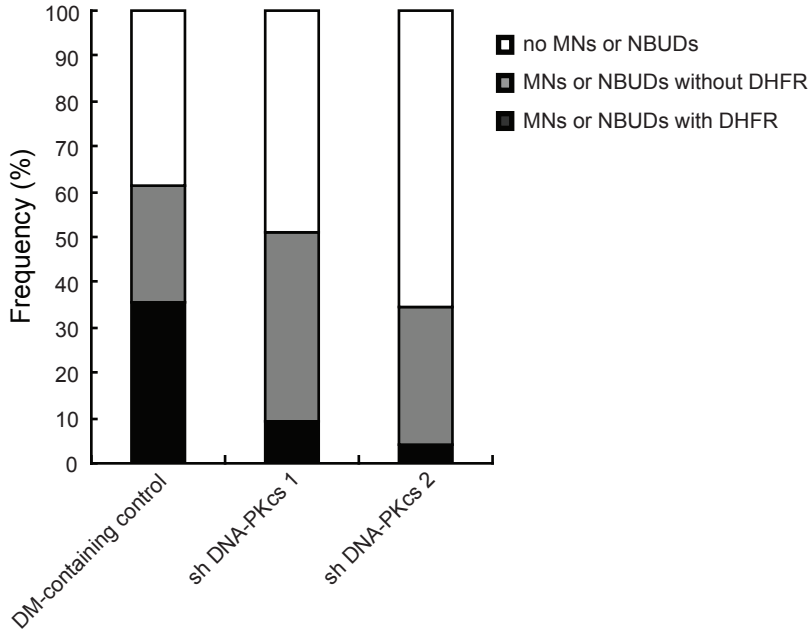
100
90
80
70
60
50
40
30
20
10
0
Frequency (%)
DM-containing control
sh DNA-PKcs 1
sh DNA-PKcs 2
no MNs or NBUDs
MNs or NBUDs without DHFR
MNs or NBUDs with DHFR

SUPPLEMENTARY FIGURE LEGENDS

Figure S1. *ZFYVE16*, *MSH3* and *DHFR* colocalized in the same (A) DMs in DM-containing cells and (B) HSRs in HSR-containing cells. The BACs used here were RP11-975J15 (*ZFYVE16*, red), RP11-90A9 (*DHFR*, green) and RP11-42H4 (*MSH3*, yellow). DAPI (blue) was used for staining chromosomes.

Figure S2. Characteristic structural features of B/F/B cycles were detected in HSR-containing cells. (A) FISH analysis of metaphase chromosomes of HSR-containing cells using FITC-labeled whole chromosome 5 probe (green) and chromosome 5-specific centromeric probe (red). DAPI (blue) was used for staining chromosomes. Dicentric chromosomes with dual centromeres of chromosome 5 were detected. The right panel is an enlarged image of the inset in the left panel. (B) Nucleoplasmic bridge observed in HSR-containing cells.

Figure S3. Depletion of DNA-PKcs in DM-containing cells caused a decrease in the formation of MNs and NBUDs. The proportion of interphase nuclei with: (i) no MNs or NBUDs, (ii) MNs or NBUDs without *DHFR* and (iii) MNs or NBUDs with *DHFR* are shown.